Graduate School of Pure and Applied Sciences

Improvement of superelastic and mechanical properties of biomedical β-Ti alloys through alloying elements adjustment and microstructure control

（合金元素調整と微細組織制御による生体用 β-Ti 合金の超弾性および機械的特性の改善）

Muhammad Farzik Ijaz

Doctoral Program in *Materials Science*
Student ID Number: 201230138
Doctor of Philosophy in *Engineering*
Advised by: Prof. Shuichi Miyazaki
Signature:

1. Introduction

Over the past several decades, Ti-Ni and Ti-6Al-4V alloys are amongst the most commercially used metallic materials for biomedical applications. The major biomedical applications of Ti-Ni alloys are in devices such as cardiovascular stents, where their superior shape-memory and superelastic effects have been successfully utilized. On the other hand, for orthopedic implant devices such as artificial hip joints Ti-6Al-4V alloy has begun to be widely used. It is because the Young's modulus of Ti-6Al-4V alloy is about half of that of the classical stainless steel alloys, which makes it reliable in variety of biomedical implant applications. Over time, despite several outstanding advantages, there have been serious health concerns regarding the use of Ti-Ni and Ti-6Al-4V alloys implants within the human body, which are apparently due to the toxic and nature of their alloying elements. As a result, wide range of new β-type Ti alloys composed of non-toxic elements have been paid more attention. However, since many of these developed β-types Ti alloys do not yet fulfill the basic attributes required for the successful biomedical implant applications. In this study we proposed that by either adjusting or exploring new alloying elements one can enhance the performance of the conventional β-type Ti-base alloys in terms of superelastic and mechanical properties required for biomedical applications. In addition, we also suggested that the suitable thermomechanical treatments are also effective in improving superelastic and mechanical properties of the β-type Ti-base alloys. It is because the superelastic recovery strain and Young's modulus of β-type Ti alloys are highly anisotropic and depends strongly on the texture and microstructure engendered during cold rolling and/or following heat treatments. Accordingly, in this study, we designed three new classes of β-Ti alloys which are potentially developed for biomedical application. At the same time from the detailed investigations, authors were intended to understand the performance and problems of conventional β-type Ti alloys. Furthermore, on the basis of current experimental findings, important remedies were also suggested to further enhance the superelastic and mechanical properties of conventional β-type Ti alloys. In the first section, of this study, the unique Sn content dependence of the critical stress for inducing martensite is discussed. This unique stress inducing martensitic transformation assisted effectively in reducing the stress hysteresis of ternary Ti-15Nb-3Mo alloy. In the second section, the effects of alloying elements and heat treatment temperature on the superelastic properties of (Ti-Zr)-Mo-Sn alloys were investigated. We suggested a new Ni-free β-type (Ti-Zr)-1.5Mo-3Sn alloy having large superelastic recovery strain value of 7% which is almost two times largest than those of other Ni-free β-type Ti alloys. This remarkable increase in the recovery strain of (Ti-Zr)-1.5Mo-3Sn alloy was explained by the evolution of desirable recrystallization texture. In the third section, a new promising class of β-Ti alloy has been developed in an attempt to replace traditional Ti-6Al-4V alloys having much higher Young's modulus value (110 GPa) than that of human bone (10-30 GPa). Thus far, in conventionally Ti-Nb-base low Young's modulus alloys such unique texture with strong $<001>_{\beta}$ orientations have not been tailored yet. Consequently, Young's moduli of Ti-Nb alloys still lie between around 40 and 80 GPa. We developed a quaternary Ti-Nb-based alloying system with novel recrystallization texture and appropriate microstructure suitable for implant applications. It was clarified that the development of novel recrystallization texture during thermal mechanical processing and less amount of omega phase are the origin for the improvement of mechanical properties in our newly developed alloy. In summary, this widespread investigation is not only beneficial to understanding the some important aspects and problems of conventional β-Ti alloys, but also introduces two novel alloying system for further improving the mechanical and superelastic properties of conventional β-Ti alloys. Accordingly, the main objective of this research is on one hand, to develop a novel alloying system as a potential substitute of the Ti-Ni alloys used in the biomedical devices and on the other hand, to suggest suitable alloying element adjustment for improving the mechanical properties such as reducing the Young's moduli of the β-Ti alloys used for the implant applications.

1. Effect of Sn addition on stress hysteresis and superelastic properties of a Ti-15Nb-3Mo alloy

The effects of Sn content on stress hysteresis and superelastic properties of Ti-15Nb-3Mo-(0-1.5)Sn were investigated. The stress hysteresis decreased with increasing Sn content due to the suppression of athermal omega phase formation. The addition of Sn was found effective for increasing superelastic recovery strain of Ti-Nb-Mo alloys.

1.1 Experimental procedures

Ti-15Nb-3Mo-(0-1.5)Sn (at.%) (all compositions are hereafter described in atomic per cent) ingots were prepared by arc-melting in an Ar atmosphere. The ingots were homogenized at 1273 K for 7.2 ks followed by cold-rolling up to 98.5% reduction in thickness. Specimens for tensile tests were cut from the as-rolled sheets by using an electric discharge cutting machine. The dimensions of the specimens were 0.14 mm in thickness and 1.5 mm in width, with a gage length of 20 mm. All specimens were heat-treated at 973 K for 0.6 ks in an Ar filled quartz tube, followed by quenching in water. Superelastic properties were characterized by loading-unloading tensile tests at room temperature (298 K). Constituent phases were investigated using an X-ray diffraction (XRD) machine. Microstructural analysis was conducted using a JEOL 2010F transmission electron microscope (TEM) operating at 200 kV.

1.2. Results and discussion

Fig. 1-1a shows stress-strain curves of Ti-15Nb-3Mo-(0-1.5)Sn alloys. The specimen was elongated until reaching 2.5% strain and then unloaded. All the alloys exhibited superelastic recovery. A single headed arrow points at the critical stress required for inducing martensitic transformation ($\sigma_{\beta\rightarrow\alpha''}$), whereas a double head arrow points at the stress where the reverse transformation finishes ($\sigma_{\alpha''\rightarrow\beta}$) upon unloading. Stress hysteresis ($\Delta\sigma$) was defined as the difference between $\sigma_{\beta\rightarrow\alpha''}$ and $\sigma_{\alpha''\rightarrow\beta}$. The Sn content dependences of $\sigma_{\beta\rightarrow\alpha''}$ and $\sigma_{\alpha''\rightarrow\beta}$ are shown in Figure 1-1b. So far, it has been reported that Sn decreases M_s of Ti-Nb based alloys. Therefore, it is expected that $\sigma_{\beta\rightarrow\alpha''}$ increases with increasing Sn content, since the stress for inducing martensitic transformation at a fixed test temperature increases with decreasing M_s of the alloy. However, Fig. 1-1b shows a peculiar Sn content dependence of $\sigma_{\beta\rightarrow\alpha''}$: it decreased by the addition of Sn up to 1 at.%, and then increased by further addition.

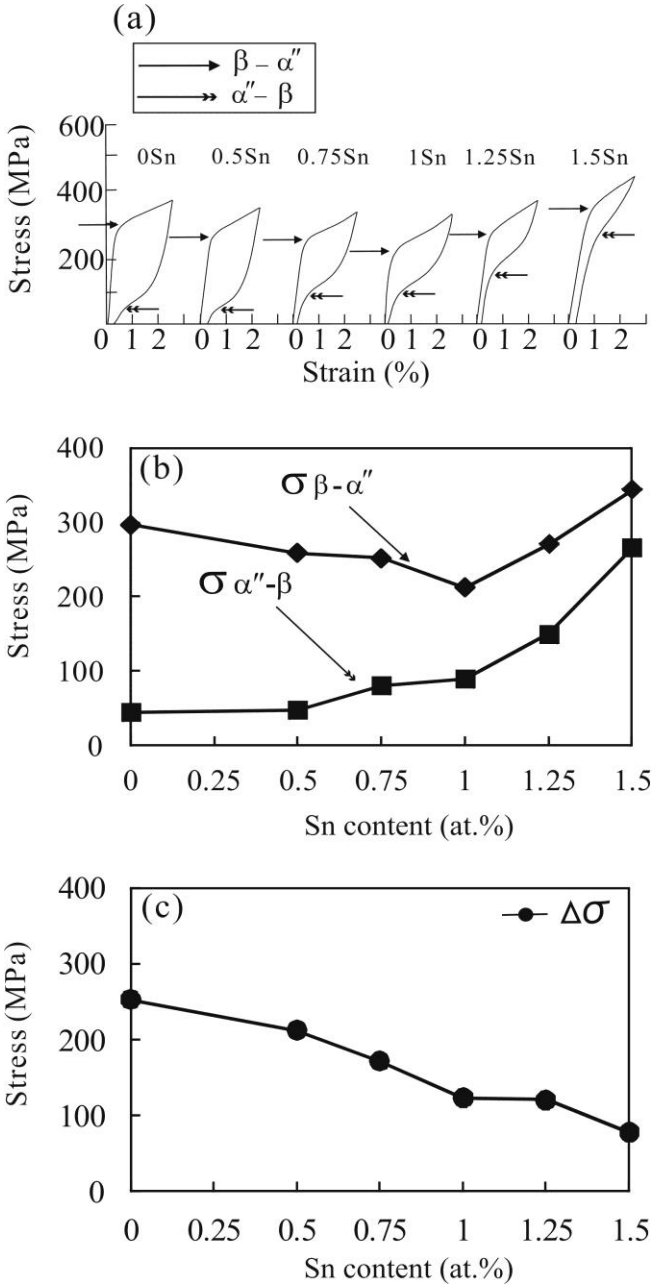

Fig. 1-1: (a) Stress-strain curves of Ti-15Nb-3Mo-(0-1.5) Sn alloys, (b) effect of Sn content on $\sigma_{\beta\rightarrow\alpha''}$ and $\sigma_{\alpha''\rightarrow\beta}$ and (c) effect of Sn content on stress hysteresis $\Delta\sigma$.

This implies that the addition of Sn up to 1 at.% raised *M*s of the Ti-15Nb-3Mo alloy, but further addition caused the decrease of M_s. On the other hand, $\sigma_{\alpha''\rightarrow\beta}$ exhibited a monotonic increasing tendency with the increase in Sn content as shown in Fig. 1b. It is important to note that the addition of Sn causes a significant decrease in $\Delta\sigma$ of the Ti-15Nb-3Mo alloy as shown in Fig. 1-1c.

1.2.1. XRD and microstructural analysis

In order to discuss the effect of Sn content on superelastic properties, XRD measurement and TEM observation were carried out. Figure 1-2a shows XRD profiles of the Ti-15Nb-3Mo-(0-1.5)Sn alloys obtained at room temperature. Within the measured 2θ (deg.) range, β phase was identified by four major reflections whereas ω phase was identified by two major reflections from $(001)_\omega$ and $(002)_\omega$. It is clearly seen that the Ti-15Nb-3Mo alloy reveals the strongest intensity of the ω phase. The peak intensities of the ω phase gradually became weaker as the Sn content increased. The peaks from the ω phase could not be detected in the XRD profiles of the Ti-15Nb-3Mo-1.25Sn and Ti-15Nb-3Mo-1.5Sn alloys. This implies that the ω phase was suppressed significantly with the increase in Sn content. The suppression of athermal omega phase (ω_{ath}) by the addition of Sn was also confirmed by TEM observation. Figure 2b shows dark-field images and the corresponding selected area diffraction patterns with zone axis of $[113]_\beta$ in the Ti-15Nb-3Mo and Ti-15Nb-3Mo-1Sn alloys. Dark-field images showing the ω phase were formed using the diffraction spot indicated by a white circle in each diffraction pattern. It is seen that the size and volume fraction of the ω_{ath} phase were remarkably reduced by the Sn addition. On the basis of microstructure analysis, the unique Sn content dependences of $\sigma_{\beta\rightarrow\alpha''}$ and stress hysteresis in the Ti-15Nb-3Mo-(0-1.5)Sn alloys can be explained by considering a two-fold role of Sn; the one hand Sn decreases *M*s of Ti-Nb based alloys, on the other hand it suppresses the ω phase formation. It has been confirmed that the athermal ω phase suppresses the martensitic transformation and increases in $\sigma_{\beta\rightarrow\alpha''}$ of Ti-Nb-Mo alloys, implying that the suppression of the athermal ω phase increases M_s. If we only consider the compositional effect, $\sigma_{\beta\rightarrow\alpha''}$ should increase monotonically with increasing Sn content because the difference between M_s and test temperature (RT) increases. However, a large amount of athermal ω phase in the Ti-15Nb-3Mo alloy decreases M_s and increases $\sigma_{\beta\rightarrow\alpha''}$ of the alloy. As mentioned above, the volume fraction of athermal ω phase decreases with increasing Sn content, indicating that the decrease in M_s due to the ω phase is reduced as the Sn content increases. Consequently the decrease in $\sigma_{\beta\rightarrow\alpha''}$ with increasing Sn content up to 1 at.% in the Ti-15Nb-3Mo-(0-1.5)Sn alloys implies the fact that the effect of Sn on the suppression of athermal ω phase is stronger than the compositional effect which decreases M_s. As the Sn content increased the effect of Sn on the suppression of athermal ω phase becomes weaker, hence the compositional effect becomes dominant. This explains why $\sigma_{\beta\rightarrow\alpha''}$ increases with increasing Sn content from 1 at.% to 1.5 at.%. On the other hand, the monotonic increase in $\sigma_{\alpha''\rightarrow\beta}$ with increasing Sn content suggests that the intrinsic compositional effect of Sn is dominant for the reverse transformation. As a result, it is believed that the monotonic change in $\sigma_{\alpha''\rightarrow\beta}$ is mainly attributed to the absence of the ω phase in the α" phase while unloading. This explains not only a large stress hysteresis loop in the ternary alloy but also the decrease of stress hysteresis with increasing Sn content.

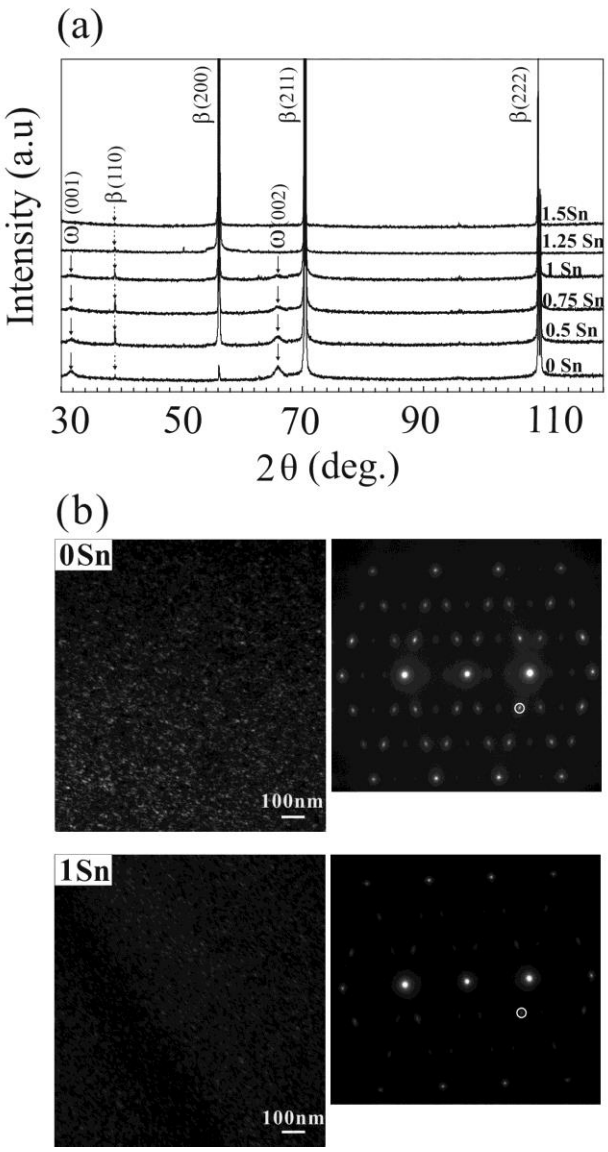

Fig 1-2: (a) XRD profiles of Ti-15Nb-3Mo-(0-1.5)Sn alloys and (b) dark field images and the corresponding selected area diffraction patterns of 0Sn and 1Sn- added

In conclusion, we are able to reduce the stress hysteresis and increase the superelastic recovery strain of a Ti-Nb-Mo alloy by the addition of Sn. The unique Sn content dependence of the critical stress for inducing martensitic transformation in Ti-15Nb-3Mo-(0-1.5)Sn alloys is due to a two-fold role of Sn, i.e. the decrease of M_s and the suppression of the athermal ω phase.

2. Superelastic properties of biomedical (Ti-Zr)-Mo-Sn alloys

A new class of β-type Ti-50Zr base shape memory and superelastic alloys was developed in order to replace Ti-Ni based alloys in the biomedical field. The (Ti-Zr)-1.5Mo-3Sn alloy exhibited excellent superelasatic properties. A large superelastic recovery strain of 7% was achieved through texture control.

2.1. Experimental procedures

Quaternary (Ti-Zr)-(1-2) at.% Mo-(2-4) at.% Sn ingots (all compositions are hereafter referred in atomic percent) were prepared by an Ar arc-melting method. The melted ingots were sealed in a vacuum in a quartz tube and homogenized at 1273 K for 7.2 ks and then air cooled. Then the ingots were cold-rolled up to 98.5% in thickness reduction. Specimens for tensile tests, X-ray diffraction (XRD) measurements, scanning electron microscopy (SEM) observation were cut using an electro-discharge machine. All the cold rolled specimens were encapsulated in quartz tubes in an Ar atmosphere and heat treated at 873, 923, 973 and 1073 K for 3.6 ks respectively, followed by quenching into water at RT without breaking the quartz tubes to mitigate oxidation. In order to investigate superelastic properties tensile tests were carried at room temperature (RT) by a tensile testing machine. The dimensions of the rectangular shaped tensile specimens were 0.15mm in thickness and 1.5mm in width, with a length of 40mm. Each tensile specimen was tested along the rolling direction, such that the tensile direction of the specimen was parallel to the rolling direction.

2.2. Results and discussion

2.2.1. Effect of annealing temperature on superelastic properties

The most stable superelasticity through alloying elements adjustment such as Mo and Sn was achieved in the (Ti-Zr)-1.5Mo-3Sn alloy composition. Therefore it was selected for further research Fig. 2-1(a)-(d) shows the results of cyclic tensile tests of (Ti-Zr)-1.5Mo-3Sn specimens heat treated at 873-1073 K for 3.6 ks. Cyclic test was done by elongating the specimen up to 2.5% strain and then removing the stress. The similar sequence of measurement was repeated by increasing maximum strain by the interval of 0.5 % (i.e. 2.5%, 3%, 3.5%..... for each successive cycle of loading) using the same specimen. In order to characterize superelastic properties quantitatively, two types of strain, i.e. recovery strain (ε_r) and remained plastic strain (ε_p) were measured at each cycle as shown in the last cycle of the specimen heat treated at 1073 K. The magnitudes of ε_r and ε_p in each cycle are plotted against maximum stress attained at each cycle for the specimens heat treated at 873-1073 K for 3.6 ks as shown in Fig. 2-2. For all the specimens, ε_p increased continuously as the maximum stress increased, whereas ε_r increased to a maximum value and then decreased. The maximum ε_r (ε_r^{max}) of each specimen is indicated with a dashed arrow in Fig. 2-2a-d. It is clearly seen that ε_r^{max} increased with increasing heat treatment temperature; from 3.8% for the specimen heat treated at 873 K to 7.0% for the specimen heat treated at 1073 K. On the other hand, the critical stress of slip (σ_{CSS}), which is defined as the stress at which 0.5% accumulative ε_p was induced during cycling, decreased monotonically from 586 MPa to 398 MPa with increasing heat treatment temperature from 873 K to 1073 K. It has been reported that low temperature annealing is an effective method to increase the superelastic recovery strain of Ti-Nb base alloys owing to a high critical stress for slip. However, the recovery strain of the (Ti-Zr)-1.5Mo-3Sn alloy increased with increasing heat treatment temperature although the critical stress for slip decreased. Fig. 2-3(a)-(d) shows $\varphi_2 = 45^\circ$ sections of ODFs obtained from specimens heat treated at 873-1073 K for 3.6 ks, respectively. The ODFs results clearly indicate a strong dependence of texture on heat treatment temperature. The specimen heat treated at 873 K exhibited a very weak texture with a maximum intensity close to $\{113\}_\beta<471>_\beta$ texture component. The specimen heat treated at 923 K revealed a maximum intensity at $\{112\}_\beta<110>_\beta$ component. In the specimen heat treated at 973 K,$\{001\}_\beta<110>_\beta$ texture component appeared in addition to the major $\{112\}_\beta<110>_\beta$ texture component. In the specimen heat treated at 1073 K, the peak intensity of the $\{001\}_\beta<110>_\beta$ texture component became very strong. It is noted that the transformation strain from the β phase to α″ phase exhibits a strong orientation dependence, and has been determined to reveal a largest value along the crystal orientation of $<110>_\beta$. Therefore, both $\{112\}_\beta<110>_\beta$ and $\{001\}_\beta<110>_\beta$ textures are favorable to the superelastic recovery strain because $<110>_\beta$ aligned along the rolling direction for both textures. As a result, it is concluded that a large superelastic recovery strain of about 7 % for the specimens heat treated at 973-1073 K for 3.6 ks is due to the strong favorable recrystallization textures, i.e. $\{112\}_\beta<110>_\beta$ and $\{001\}_\beta<110>_\beta$, in addition to the large transformation strain

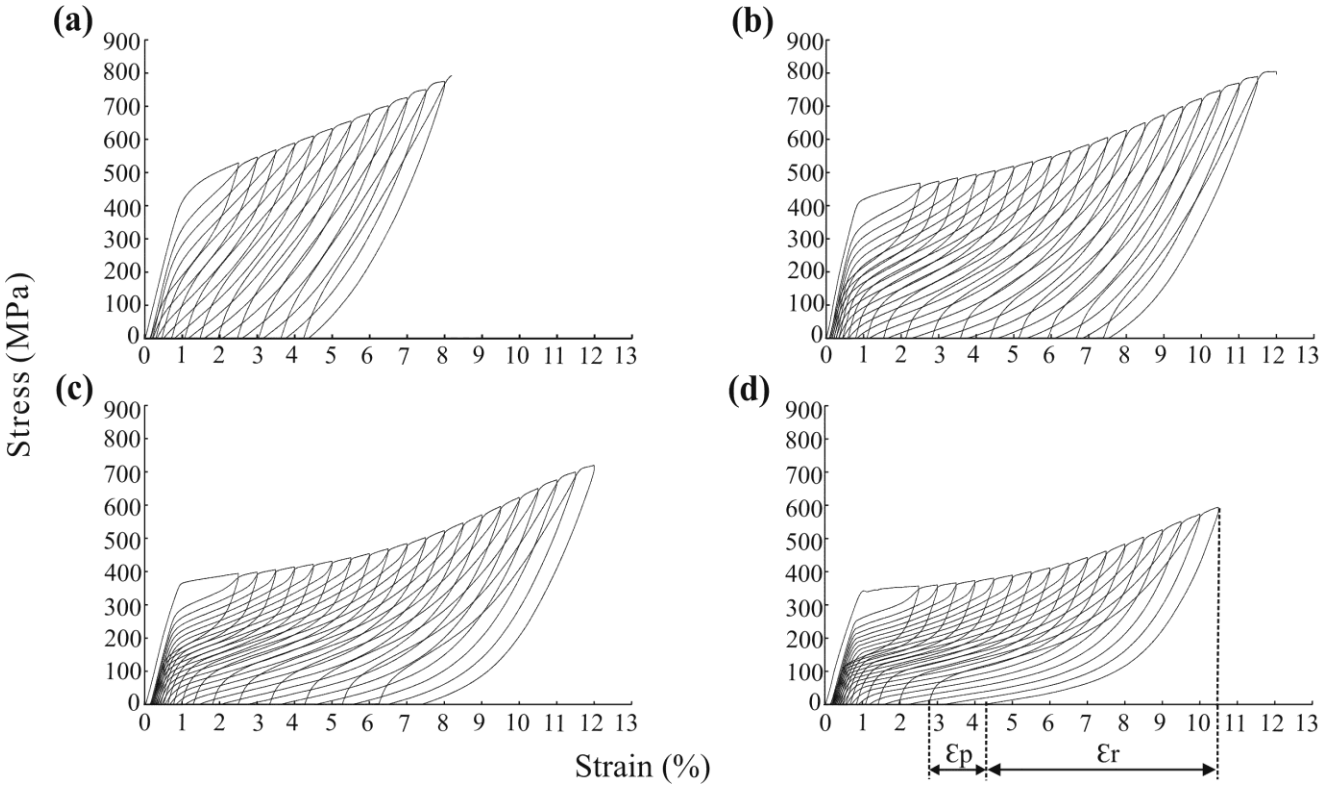

Fig. 2-1: Stress-strain curves obtained by cyclic loading-unloading tensile test for the specimens heat treated at: (a) 873 K , (b) 923 K, (c) 973 K and (d) 1073 K for 3.6 ks.

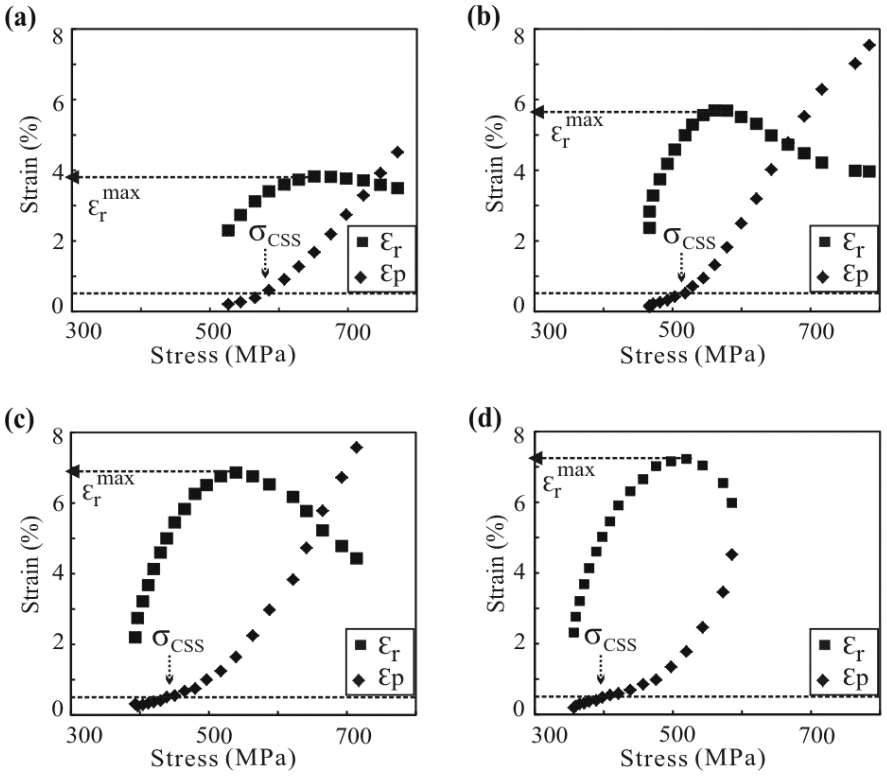

Fig. 2-2: Plastic and superelastic recovery strains as a function of the maximum stress attained during cycling for the specimens heat treated at ; (a) 873 K , (b) 923 K, (c) 973 K and (d) 1073 K for 3.6 ks.

2.2.2. Microstructural characterization

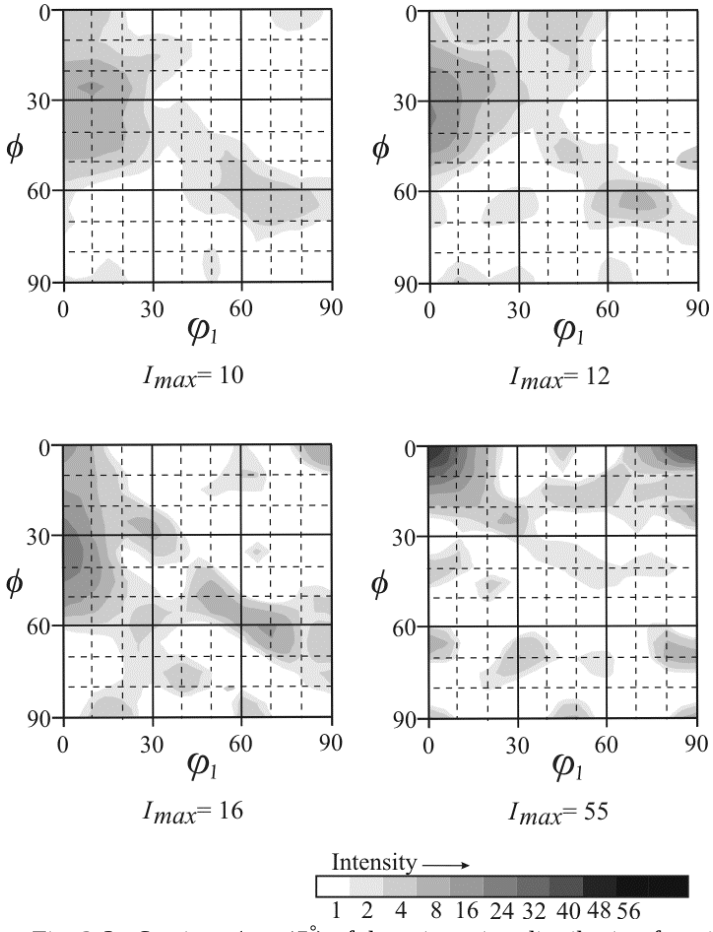

Fig. 2-3: Sections (φ_2=45°) of the orientation distribution functions for the specimens heat treated at (a) 873 K, (b) 923 K, (c) 973 K and (d) 1073 K for 3.6 ks.

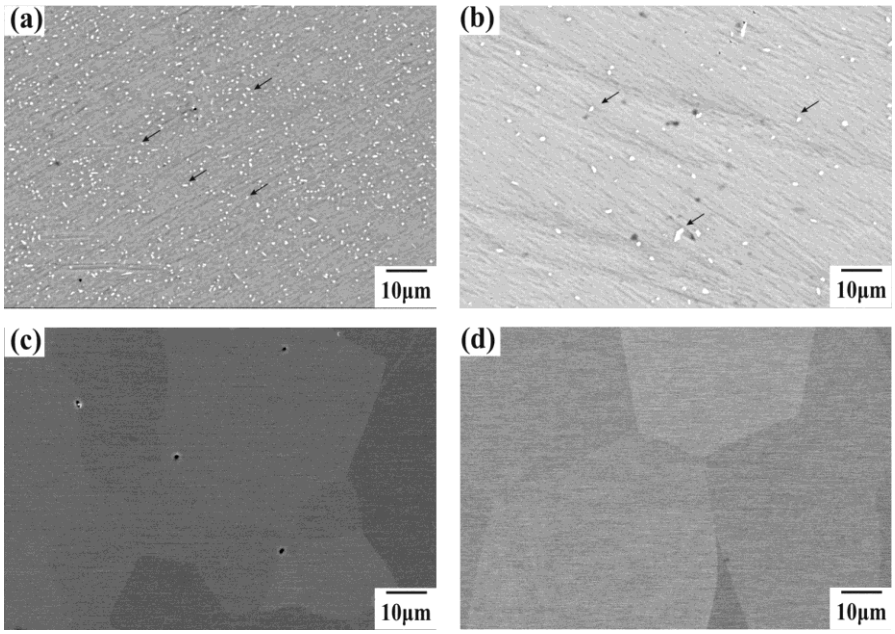

Fig. 2-4: Back-scattered SEM images of the specimens heat treated at (a) 873 K, (b) 923 K, (c) 973 K and (d) 1073 K for 3.6 ks

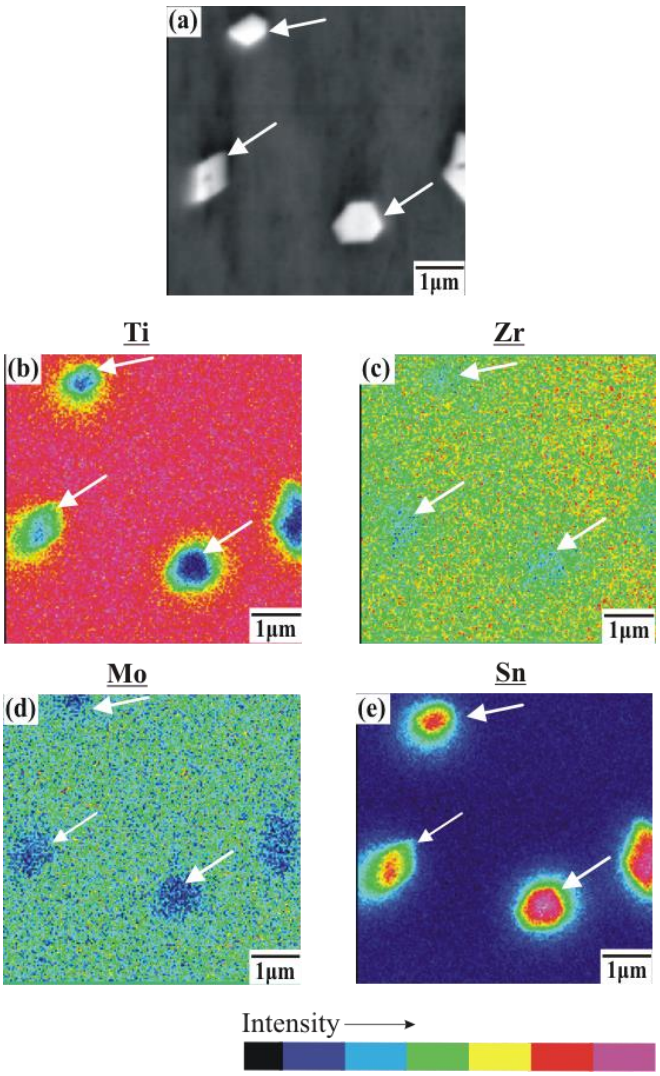

Fig. 2-5: X-ray mapping images of the specimen heat treated at 923 K indicating the elemental distribution of alloying elements.

Fig.2-4(a)-(d) shows scanning electron images of the (Ti-Zr)-1.5Mo-3Sn specimens heat treated at temperatures between 873-1073 K for 3.6 ks. For the specimens heat treated at 873 K and 923 K, the secondary phase can be seen as relatively white precipitates on the image. However, in the specimen heat treated at 973 K, the precipitates were rarely observed. On the other hand, in the case of the specimen heat treated at 1073 K, the secondary phase could not be detected as shown in Fig. 2-4(d). EPMA mapping results of the precipitates observed in the specimen heat treated at 923 K with respect to alloying elements are shown in Fig. 2-5(a)-(d). Fig. 2-5(b) and 2-5(d) show that the concentrations of Ti and Mo are lower in the precipitates when compared with surrounding matrix. Fig. 2-5(e) also reveals that the Sn content in the precipitates is higher when compared to matrix. It is also seen that Zr is slightly rich in the precipitates. Fig.2-6(a)-(d) shows XRD profiles of the (Ti-Zr)-1.5Mo-3Sn specimens heat treated at temperatures between 873-1073 K for 3.6 ks. From the XRD profile of the specimen heat treated at 873 K additional peaks along with β phase could be identified as Zr_5Sn_3 phase, as is consistent with EPMA results. As a result, it is suggested that the dissolution of Zr_5Sn_3 precipitates at temperatures higher than 973 K leads to the grain growth and formation of strong recrystallization textures. In conclusion a new class of β-Ti alloys is introduced in this research; especially the superelastic recovery strain of (Ti-Zr)-Mo-Sn increases significantly with increasing heat treatment temperature and showed a remarkable recovery strain of 7% which is found to be two times larger than the other conventional β-Ti-based superelastic alloys reported so far. This remarkable increase in the recovery strain of (Ti-Zr)-1.5Mo-3Sn alloy was explained by the evolution of desirable recrystallization texture during thermomechanical treatments.

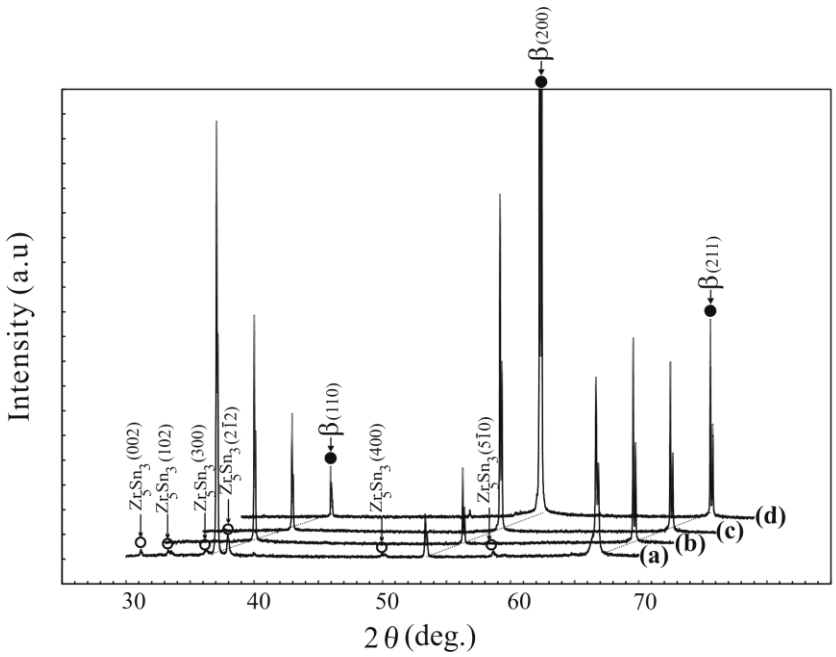

Fig. 2-6: XRD profiles of the specimens heat treated at; (a) 873 K, (b) 923 K, (c) 973 K and (d) 1073 K for 3.6 ks.

3. Effect of Sn content on microstructures and mechanical properties of quaternary β-Ti alloy for implant applications

In order to, alleviate the outstanding stress shielding problem associated to conventional Ti-6Al-4V alloy as a result of large mismatches among the Young's moduli at the at the human bone/implant interface a new low Young's moduli biomedical β-type Ti-Nb-base alloys have been developed. This research study also systematically explored the strategies for the enhancement of mechanical biocompatibility of our newly developed β-Ti alloys. Specifically, in the area of mechanical biocompatibility the improvement of mechanical properties by reducing the Young's moduli are the key aspects required for the successful of new biomedical alloys to be used for orthopedic implant applications. Therefore in this study special attention has been paid to improve the mechanical properties through suitable alloying element adjustments and by tailored heat treatment methods which are targeted to control the recrystallization texture and microstructures of our newly developed β-Ti alloys.

3.1. Experimental procedure

A series of β-type Ti-Nb-based (at.%) alloy ingots were prepared by an Ar arc-melting method The button-shaped arc melted ingots were homogenized at 1273 K for 7.2 ks in vacuum, after which they were air cooled. Then ingots were cold-rolled in to sheets with a reduction of 95%. The cold rolled specimens were subjected to solution treatment (ST) at 1073 K for 1.8 ks, and then were quenched in to water. To deeply characterize the phase constituents of the samples were also systematically investigated by XRD at room temperature. Orientation distribution function (ODFs) was constructed while using three pole figures. Finally, TEM observations were conducted on a JEOL 2010F instrument operated at 200 kV. For the sake of maximum accuracy the Young's modulus values of the specimens of each alloy were measured by using a free resonance method.

3.2 Results and discussions

Experimental results have conclusively revealed that the simultaneous development of both recrystallization texture and suitable microstructures during heat treatment are highly beneficial for reducing the Young's moduli of our newly prepared β-type Ti-Nb based alloys and are also advantageous for improving the mechanical properties of conventional β-Ti alloys.. In conclusion, the results demonstrated that the Young's modulus values of our newly developed β-Ti alloys prepared by an arc melting method are highly anisotropic and indicated strong dependence on the microstructures developed during heat treatment. In particular, the attractive combination of attributes like low Young's modulus value and higher ultimate tensile strength, while simultaneously keeping the advantage of fabrication ease makes our newly developed β-type Ti-Nb-based alloy as a viable candidate for the future biomedical implant applications.